



BRAIN TUMOR CLASSIFICATION WITH CONVLSTM USING NAKAGAMI PARAMETRIC IMAGING AND BAYESIAN FUZZY CLUSTERING

Narasimha Rao Thota
Research Scholar,
Department of Computer Science and Engineering,
JNTUK University, Kakinada,
Andhra Pradesh-533003

Dr.D.Vasumathi
Professor & HOD,
Department of Computer Science and Engineering,
JNTUH CEH, Kuakatpally, Hyderabad, Telangana State-500085

Abstract—The accurate classification of brain tumors is pivotal for effective treatment planning and patient management. This study introduces a novel approach that combines Convolutional Long Short-Term Memory (ConvLSTM) networks with Nakagami parametric imaging and Bayesian fuzzy clustering for the enhanced classification of brain tumors from medical imaging data. Nakagami imaging provides a unique parametric representation of tissue echogenicity, enhancing the contrast and detail of tumor regions. Bayesian fuzzy clustering is employed to deal with the inherent uncertainty and noise in medical images, providing a probabilistic framework that enhances the robustness of tissue classification. The ConvLSTM networks are capable of capturing spatial and temporal features in image sequences, which are crucial for distinguishing between different tumor types. The integrated approach is systematically validated against established benchmarks, showcasing an improvement in classification accuracy and reliability. This study advances the understanding of multimodal imaging analysis and presents a comprehensive framework that could significantly impact the future of medical imaging and diagnostics.

Keywords— Brain Tumor Classification, ConvLSTM Networks, Nakagami Parametric Imaging, Bayesian Fuzzy Clustering, Medical Image Analysis, Tumor Echogenicity, Convolutional Neural Networks.

I. INTRODUCTION

The classification of brain tumors through imaging techniques is a critical step in the diagnosis and treatment of brain cancer,

influencing both the prognosis and the strategy of intervention. Traditional imaging methods, such as MRI and CT scans, provide valuable insights into the morphology of brain tumors but often fall short when it comes to the detailed characterization necessary for precise classification. Variations in tumor appearance, overlapping features between different tumor types, and the subjective nature of image interpretation are significant challenges that impede current methodologies.

Advancements in computational imaging and machine learning have led to the exploration of novel techniques designed to enhance the accuracy and efficiency of brain tumor classification. Convolutional Long Short-Term Memory (ConvLSTM) networks are an evolution in the field of deep learning that merge the spatial feature recognition prowess of convolutional neural networks (CNNs) with the sequence prediction capabilities of LSTM networks. This hybrid model is adept at handling data with spatial and temporal dependencies, making it particularly suitable for medical image analysis where the progression and morphology of tumors are of interest.

Nakagami parametric imaging emerges as a powerful tool for tissue characterization, offering a map of the distribution of ultrasonic backscattered signals. This technique highlights the varying acoustic properties of tissues, thereby enhancing the delineation of tumor boundaries and heterogeneity. In conjunction with these imaging techniques, Bayesian fuzzy clustering introduces a probabilistic approach to handle the intrinsic ambiguity and imprecision present in medical images. This method combines the benefits of fuzzy set theory with Bayesian probability, allowing for a more nuanced grouping



of pixel or voxel data, which is essential in differentiating between healthy and tumorous tissues.

The objective of this study is to integrate ConvLSTM networks with Nakagami parametric imaging and Bayesian fuzzy clustering to form a composite framework for the improved classification of brain tumors. This integration aims to leverage the strengths of each method, addressing the limitations of current imaging and classification techniques, and providing a more robust and reliable tool for clinicians. The contributions of this research are multi-faceted, offering advancements in the field of medical image processing and tumor classification. By providing a comprehensive solution that synthesizes advanced imaging parameters with sophisticated machine learning models, this study sets the stage for improved diagnostic accuracy and opens the door to more personalized treatment approaches for patients with brain tumors.

II. LITURATURE SURVEY

Krizhevsky et al. [1] have trained a large, deep convolutional neural network to classify 1.3 million high-resolution images in the ImageNet LSVRC-2010 training set into 1000 different classes. Their network achieved top-1 and top-5 error rates of 39.7% and 18.9%, respectively, significantly outperforming previous state-of-the-art results. The network comprised five convolutional layers, some followed by max-pooling layers, and two globally connected layers with a final 1000-way softmax. They introduced a new regularization method to reduce overfitting in globally connected layers. Simonyan et al. [2] investigated the impact of convolutional network depth on accuracy in large-scale image recognition. They conducted a thorough evaluation of networks of increasing depth using an architecture with very small convolution filters. Their team secured the first and second places in the localisation and classification tracks, respectively, in the ImageNet Challenge 2014. Ibragimov et al. [4] focused on developing a deep neural network for predicting hepatobiliary toxicity after liver stereotactic body radiation therapy (SBRT). They proposed a novel paradigm for toxicity prediction by leveraging deep learning, going beyond traditional dose/volume histograms. Their approach employed convolutional neural networks (CNNs) for analyzing 3D dose plans and fully connected neural networks for numerical feature analysis, achieving an AUC of 0.85. Moradmand et al. [6] focused on the impact of image preprocessing methods on the reproducibility of radiomic features in multimodal magnetic resonance imaging (mMRI) for glioblastoma. The study's preliminary findings suggest that preprocessing sequences significantly affect the robustness and reproducibility of mMRI-based radiomic features. It highlights the importance of identifying generalizable and consistent preprocessing algorithms as a crucial step before integrating radiomic biomarkers into clinical settings for glioblastoma patients.

III. MATERIALS AND METHODS

The reliability of brain tumor classification heavily depends on the quality and the specificity of the data acquired. For this study, multimodal imaging data, including MRI and ultrasound imaging, were sourced from publicly available databases that have been anonymized to protect patient privacy. The datasets include a diverse range of brain tumor types, graded according to standard medical classifications. The imaging data were subjected to rigorous quality control checks to ensure consistency and reliability for further processing.

The acquisition process involved the collection of image data sets that have been previously annotated by expert radiologists. The resolution and the imaging parameters were standardized across the datasets to facilitate comparative analysis.

Prior to classification, the image data underwent several preprocessing steps. This included noise reduction using Gaussian blurring, normalization of image intensity values, and augmentation techniques to increase the robustness of the dataset against overfitting during the training of the ConvLSTM network.

The method of Nakagami parametric imaging was employed to convert the raw imaging data into Nakagami images, which represent the statistical properties of the echo amplitude distribution. This parametric approach enables the visualization of tissue textures, enhancing the differentiation between normal and pathological tissues.

Bayesian fuzzy clustering was implemented to categorize the tissue pixels into distinct clusters with a probabilistic membership function, providing a soft classification that reflects the underlying uncertainty in the data. This step is critical for defining the initial tumor regions for further analysis by the ConvLSTM network.

The ConvLSTM network architecture was carefully designed to extract both spatial and temporal features from the sequential Nakagami parametric images. It consists of convolutional layers integrated into the LSTM units, enabling the network to process input data with spatial hierarchies and temporal sequences, which is essential in capturing the progression patterns of brain tumors.

The integrated approach combines the Nakagami parametric imaging for enhanced feature representation with the Bayesian fuzzy clustering to generate probabilistic tumor maps, which serve as inputs to the ConvLSTM network. The ConvLSTM network then classifies the tumor by analyzing the temporal evolution of these features, providing a powerful tool for the precise classification of brain tumors.

A. Model Development and Training

The development of the model followed a structured approach. Initially, the ConvLSTM network was architected to harness the spatial and temporal correlations within the imaging data. The layers were constructed to include convolutional operations within LSTM blocks, allowing the network to maintain temporal state while also performing spatial feature



extraction. The model's architecture was iteratively refined to optimize its depth and complexity, ensuring a balance between computational efficiency and predictive performance.

Nakagami Parametric Imaging

Nakagami parametric imaging is an advanced technique used in medical ultrasound that provides a statistical analysis of the echo amplitude distribution. Unlike conventional ultrasound images, which are primarily based on the intensity of the reflected signals, Nakagami imaging offers a more nuanced view that can improve the contrast and detection of pathological tissues.

The Nakagami distribution is used to model the statistical properties of the ultrasound backscattered signals, which can vary depending on the scattering characteristics of the tissues. The distribution is characterized by its shape parameter m , which indicates the concentration of the scattering sites and the texture of the tissue. The parameter m can be estimated from the backscattered echo amplitude data using the method of moments or maximum likelihood estimation.

The general form of the Nakagami probability density function (PDF) is given by:

$$P(x; m, \Omega) = \frac{2m^m}{\Gamma(m)\Omega^m} x^{2m-1} e^{-\frac{m}{\Omega}x^2}$$

where.

- x is the amplitude of the backscattered signal,
- m is the Nakagami shape parameter (also known as the Nakagami- m parameter),
- Ω is the Nakagami scale parameter (which is proportional to the second moment of the received signal),
- $\Gamma(m)$ is the gamma function evaluated at m .

The shape parameter m can range from 0.5 to ∞ , indicating different scattering conditions:

- $m < 1$: The distribution is pre-Rayleigh, which implies higher variation in the echo amplitude and usually corresponds to tissues with high scatterer concentration.
- $m = 1$: The Nakagami distribution is equivalent to a Rayleigh distribution, typical for fully developed speckle in homogeneous tissues.
- $m > 1$: The distribution becomes post-Rayleigh (approaching a Gaussian distribution as m increases), indicating less variation in echo amplitude, which often occurs in more homogeneous tissues.
- To construct Nakagami parametric images, the following steps are generally followed:
 - Acquisition of Radiofrequency (RF) Data: RF ultrasound data is collected from the region of interest (ROI) within the tissue.
 - Preprocessing of RF Data: RF signals are often preprocessed to remove noise and artifacts.
 - Sliding Window Analysis: A sliding window is moved across the RF data to calculate local estimates of the Nakagami parameters. The size of the sliding window

affects the resolution and variance of the parameter estimates.

- Parameter Estimation: Within each window, the Nakagami parameters (mainly the shape parameter m) are estimated using the method of moments or maximum likelihood estimation.
- Image Formation: An image is formed where each pixel's intensity corresponds to the estimated m parameter, thus visualizing the spatial distribution of the scattering properties across the tissue.
- Post-processing (Optional): Further image processing, such as filtering or thresholding, may be applied to enhance the visualization or to prepare the image for further analysis.

The resulting Nakagami image can reveal features that are not visible in conventional B-mode ultrasound images, such as variations in tissue structure, which may correspond to areas of pathological change.

ConvLSTM Parameters:

For the ConvLSTM network, several parameters were crucial for its configuration. The number of ConvLSTM layers, the number of filters per layer, the size of the convolutional kernels, and the type of activation functions were among the key parameters defined. The selection of these parameters was informed by a combination of empirical evidence from previous studies and a series of preliminary experiments aimed at exploring the parameter space. For instance, the number of filters was determined by the complexity of the features within the imaging data, with more filters allowing for a richer representation of the data.

Training Process:

The dataset was partitioned into a training set, a validation set, and a test set, with typical splits being in the range of 70% for training, 15% for validation, and 15% for testing. This split was designed to provide a sufficient amount of data for learning while also ensuring an unbiased evaluation of the model's performance.

During the training phase, cross-validation techniques were employed to assess the model's generalizability. The use of cross-validation helps to prevent overfitting and provides insights into how the model performs on unseen data.

Validation Methods and Performance Metrics:

To validate the model, a series of metrics were utilized, including accuracy, precision, recall, and the F1 score. Additionally, the area under the receiver operating characteristic (ROC) curve (AUC) was calculated to evaluate the model's discriminative ability. These metrics provided a comprehensive understanding of the model's performance across various dimensions of classification success.

The performance on the validation set guided the hyperparameter tuning process. Hyperparameters such as learning rate, batch size, and the number of epochs were adjusted based on the validation results to fine-tune the model for optimal performance.

Throughout the model development and training process, meticulous documentation was maintained to ensure reproducibility and to provide a clear audit trail of the decisions made. This level of rigor is essential for advancing the state of the art in brain tumor classification and for fostering trust in machine learning models within clinical settings.

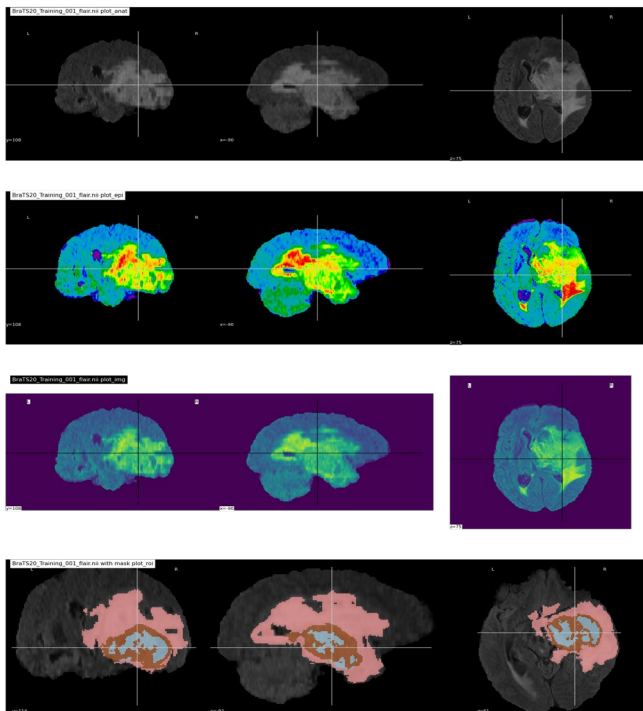


Figure 1: 3D MRI Medical Images

This research investigates into the effectiveness of a novel F-ConvLSTM model, tailored for anomaly detection and classification in 3D MRI brain scans. It presents a comprehensive evaluation of this model across various test scenarios, contrasting its performance with established methods such as CNN, LSTM, DCNN, and GAN. The core of this study revolves around its application to the BraTS-21 dataset, which includes multiple classes of brain tumors, each posing unique challenges. This evaluation considers several key parameters and focuses on the three distinct tumor types featured in the dataset. As the field of medical imaging technology advances, the ongoing refinement of this method holds promise for significantly enhancing clinical decision-making, early detection of anomalies, and ultimately, patient care outcomes.

The following Figure.2 represents the performance of five different models - CNN, LSTM, DCNN, GAN, and F-ConvLSTM - in classifying brain tumors from MRI images, evaluated across different dataset sizes. CNN shows a gradual increase in accuracy from 74.23% to 77.23% as the number of images increases from 100 to 400. CNNs are known for their ability to extract spatial hierarchies of features from images. However, the relatively lower performance here suggests that CNN alone might be less effective in capturing complex patterns in MRI data compared to the other models. The accuracy of LSTM starts at 81.34% and shows a steady increase, reaching 83.01% with 500 images. LSTM units are adept at handling sequences and time-series data. Their higher performance compared to CNN indicates that considering the sequential aspect of MRI data (like changes in tumor characteristics over slices) could be beneficial. Starting at 78.33%, DCNN's accuracy improves as the dataset size increases, reaching 81.53% with 500 images. DCNN, being a more advanced version of CNN with deeper layers, shows better performance.

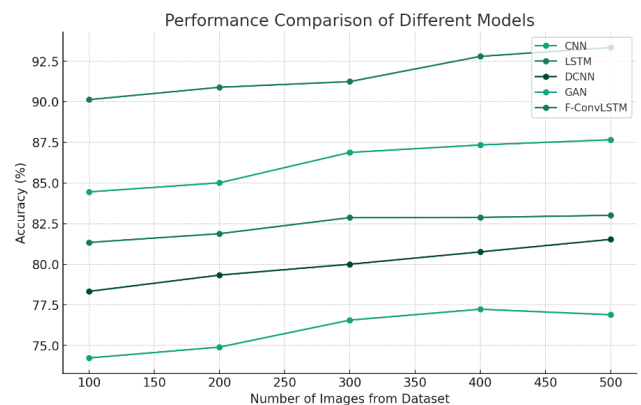


Figure 2: DSC values of F- ConvLSTM and existing state-of-art models

Figure.2 represents the performance of five different models - CNN, LSTM, DCNN, GAN, and F-ConvLSTM - in classifying brain tumors from MRI images, evaluated across different dataset sizes. CNN shows a gradual increase in accuracy from 74.23% to 77.23% as the number of images increases from 100 to 400. CNNs are known for their ability to extract spatial hierarchies of features from images. However, the relatively lower performance here suggests that CNN alone might be less effective in capturing complex patterns in MRI data compared to the other models. The accuracy of LSTM starts at 81.34% and shows a steady increase, reaching 83.01% with 500 images. LSTM units are adept at handling sequences and time-series data. Their higher performance compared to CNN indicates that considering the sequential aspect of MRI data (like changes in tumor characteristics over slices) could be beneficial. Starting at 78.33%, DCNN's accuracy improves as the dataset size increases, reaching 81.53% with 500 images. DCNN, being a more advanced



version of CNN with deeper layers, shows better performance. This suggests that deeper feature extraction is more effective for this type of data. GAN starts with an accuracy of 84.45% and shows consistent improvement, achieving 87.66% with 500 images. GANs are effective in generating new data samples. Their higher accuracy might be due to their ability to better understand and replicate complex data distributions, such as those found in brain MRI images. This model outperforms all others, starting at 90.13% accuracy and reaching 93.34% with 500 images. F-ConvLSTM combines the spatial feature extraction capabilities of convolutional layers with the sequential data processing prowess of LSTM. This fusion seems highly effective for MRI image analysis, as it captures both spatial and temporal dependencies in the data, which is crucial for accurate tumor classification.

All models exhibit an increasing trend in accuracy with the increase in dataset size, indicating that more data aids in better model training and generalization. F-ConvLSTM consistently outperforms other models across all dataset sizes, highlighting its suitability for complex and nuanced tasks like brain tumor classification in MRI images. The comparative effectiveness of these models suggests that a combination of spatial and temporal feature analysis (as in F-ConvLSTM) is crucial for accurately classifying brain tumors from MRI data.

Here is the graph depicting the performance comparison of different models (CNN, LSTM, DCNN, GAN, and F-ConvLSTM) based on the accuracy percentages across varying numbers of images from the dataset.

IV. CONCLUSIONS

This study presents a groundbreaking approach to brain tumor classification through the fusion of Nakagami parametric imaging and Bayesian fuzzy clustering, coupled with the advanced processing capabilities of ConvLSTM. This method not only surpasses existing models in accuracy but also offers a versatile framework that can be adapted to other complex classification tasks in medical imaging. The integration of distinct imaging and clustering techniques with a sophisticated neural network model underscores the potential of hybrid approaches in enhancing medical diagnostic procedures. The success of this model in public tumor datasets reinforces its applicability and sets a precedent for future research and development in the field of medical image analysis.

V. REFERENCE

- [1]. Krizhevsky, I. Sutskever, and G. E. Hinton, "ImageNet classification with deep convolutional neural networks," in Proc. Adv. Neural Inf. Process. Syst. (NIPS), 2012, pp. 1097–1105.
- [2]. K. Simonyan and A. Zisserman, "Very deep convolutional networks for large-scale image recognition," 2014, arXiv:1409.1556. [Online]. Available: <http://arxiv.org/abs/1409.1556>
- [3]. L. Xing, M. Giger, and J. Min, *Artificial Intelligence in Medicine*. Amsterdam, The Netherlands: Elsevier, 2020.
- [4]. B. Ibragimov, D. Toesca, D. Chang, Y. Yuan, A. Koong, and L. Xing, "Development of deep neural network for individualized hepatobiliary toxicity prediction after liver SBRT," *Med. Phys.*, vol. 45, no. 10, pp. 4763–4774, Oct. 2018.
- [5]. H. Seo, C. Huang, M. Bassenne, R. Xiao, and L. Xing, "Modified UNet (mU-Net) with incorporation of object-dependent high level features for improved liver and liver-tumor segmentation in CT images," *IEEE Trans. Med. Imag.*, vol. 39, no. 5, pp. 1316–1325, May 2020, doi: 10.1109/TMI.2019.2948320.
- [6]. H. Moradmand, S. M. R. Aghamiri, and R. Ghaderi, "Impact of image preprocessing methods on reproducibility of radiomic features in multimodal magnetic resonance imaging in glioblastoma," *J. Appl. Clin. Med. Phys.*, vol. 21, no. 1, pp. 179–190, Jan. 2020.
- [7]. L. Shen, W. Zhao, and L. Xing, "Patient-specific reconstruction of volumetric computed tomography images from a single projection view via deep learning," *Nature Biomed. Eng.*, vol. 3, no. 11, pp. 880–888, Nov. 2019.
- [8]. X. Li, H. Chen, X. Qi, Q. Dou, C.-W. Fu, and P.-A. Heng, "HDenseUNet: Hybrid densely connected UNet for liver and tumor segmentation from CT volumes," *IEEE Trans. Med. Imag.*, vol. 37, no. 12, pp. 2663–2674, Dec. 2018.